34th EPS Conference on Plasma Phys. Warsaw, 2 - 6 July 2007 ECA Vol.31F, P-1.040 (2007)

Simulating divertor detachment of ohmic discharges in ASDEX Upgrade using SOLPS: the role of carbon

M. Wischmeier[1], D. Coster[1], A. Chankin[1], C. Fuchs[1], M. Groth[3], J. Harhausen[1], A. Kallenbach[1], H.W. Müller[1], M. Tsalas[2], E. Wolfrum[1] and ASDEX Upgrade team

[1] *Max-Planck-Institut für Plasmaphysik, EURATOM-Association, Garching, Germany,*

[2] *NCSR "Democritos", Inst. of Nucl. Technology Rad. Prot., Attica, Greece*

[3] *Lawrence Livermore National Laboratory, Livermore, California, USA*

Introduction

With divertor detachment being a prerequisite for burning plasma operation in ITER, numerical codes such as SOLPS [1] have been developed for predicting and interpreting the divertor performance at all operational regimes in current tokamaks and ITER. In ITER complete detachment from the outer divertor target is not permitted as this might result in an X-point MARFE, imposing an upper limit for the upstream separatrix density, n_e^{sep}. Despite the knowledge of the basic mechanisms required for achieving detachment, such as radiative power exhaust, volumetric momentum and charge removal [1], a quantitative evaluation of experimentally observed detached regimes proves to be difficult for several tokamaks. In particular the strong asymmetry of the ion flux density between the inner, Γ_{it}, and the outer target, Γ_{ot}, with increasing line averaged density, $\bar{n}_e$, and the 'vanishing' of the ion flux, defined as full/complete detachment, at the inner target cannot be reproduced. It is unclear how this is related to divertor target plates or other plasma facing components containing carbon. As part of a combined effort at various experimental devices this paper contributes to the validation of the SOLPS code against experimental data from ASDEX Upgrade, AUG, at the onset of divertor detachment. In the framework established under the International Tokamak Physics Activity (ITPA) Divertor and SOL working group a series of ohmic discharges have been performed in AUG, which had as similar as possible plasma parameters as companion discharges undertaken in DIII-D [2]. The effect of activating drift terms, the influence of the chemical sputtering yield at the inner target and the role of impurity influx from the inner heat shield are analyzed based on results presented in [3].

Experiment

The presence of ELMs is avoided by concentrating on ohmic discharges in lower single null configuration in AUG with the divertor IIb and vertical targets. In 2006, the plasma facing components, PFCs, in the divertor strike zones were made of graphite, whilst the majority of the other PFCs were covered by tungsten [4]. The cryogenic pumps were active in all discharges, with $I_p = 1.0MA$, $B_T = -2.0T$ and $q_{95} = 3.4$ and the ion ∇B direction pointed downwards, the forward field direction. The discharges covered $\bar{n}_e$ from $2.7 \times 10^{19} m^{-3}$ to $6.5 \times 10^{19} m^{-3}$ with the heating power varying accordingly between $500kW$ and $800kW$. The same magnetic configuration was used for all discharges (see also Fig.2). In order to resolve the plasma profiles along the target, the strike point was swept. In this paper, partial detachment is defined as a reduction of Γ_t locally with increasing $\bar{n}_e$, combined with a loss of plasma pressure between upstream and

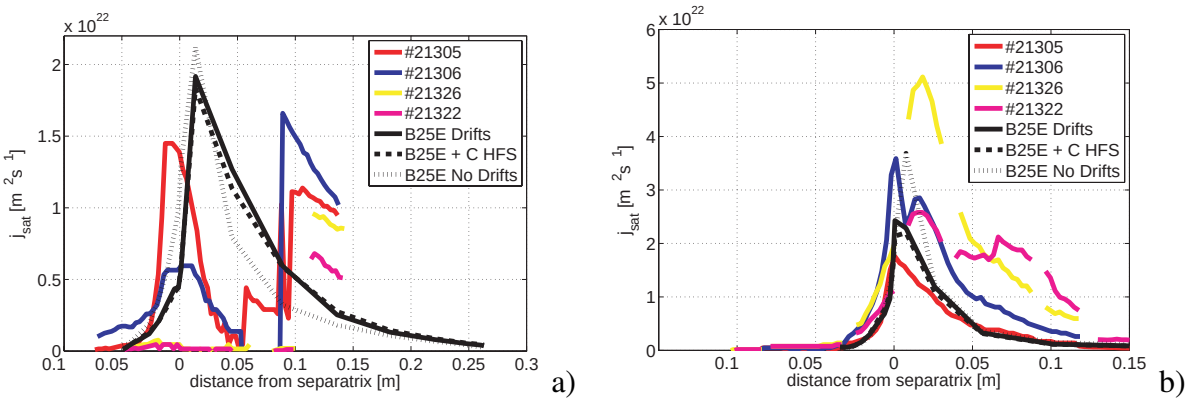

Figure 1: *Ion flux densities to the inner (a) and outer targets (b) derived from the ion saturation currents of the fixed Langmuir probes for the discharges* #21305 *at* $\bar{n}_e = 2.7 \times 10^{19} m^{-3}$, #21306 *at* $\bar{n}_e = 3.8 \times 10^{19} m^{-3}$, #21326 *at* $\bar{n}_e = 5.5 \times 10^{19} m^{-3}$ *and* #21322 *at* $\bar{n}_e = 6.5 \times 10^{19} m^{-3}$, *together with simulations (black, B25E) for the lowest density case (red curve).*

target locations by more than a factor 2 (assuming Mach ≥ 1 at the target). Complete detachment occurs if Γ_t falls to very low levels along the entire target. In Fig. 1 the measured profiles of Γ_t along the inner (a) and outer targets (b) are presented. The far SOL profiles at the inner target are not an artefact but a consequence of the divertor geometry. The inner target peak ion flux, Γ^{it}_{pk}, decreases with increasing $\bar{n}_e$, whilst at the outer target, Γ^{pk}_{ot} at first increases and then decreases as a function of $\bar{n}_e$ (known as 'roll over'). At the same time the inner target is initially partially detached and reaches complete detachment at the highest $\bar{n}_e$. At the lowest density both targets have a similar Γ^{pk}, however, with increasing $\bar{n}_e$ they rapidly differ by an order of magnitude.

Modelling

The SOLPS5.0 code package [1] is applied, using the fluid code B2.5 coupled to the neutrals Monte Carlo Code EIRENE (version '99) with all drift terms being activated. Despite the earlier version of the code (SOLPS4.0/4.2, no drift terms included) has been and is being used for predicting the operational regime of ITER and successfully demonstrated qualitatively partially detached solutions, there are difficulties in matching experimental results *quantitatively* in the high recycling and detached regimes. The modelling here focuses on the lowest experimental $\bar{n}_e$ in which $n_e^{sep} \sim 0.8 - 1.0 \times 10^{19} m^{-3}$, equivalent to $\sim \bar{n}_e/3$, with the aim of investigating the experimentally observed highly asymmetric divertor with respect to Γ_t as a function of $\bar{n}_e$. For simulating a large set of parameters, a grid with a relatively low resolution as shown in Fig. 2 with 48 poloidal and 18 radial cells has been used. The power entering the computational domain was varied between $520kW$ and $700kW$. A gas puff of $\sim 6.5 \times 10^{20} s^{-1}$ and a pumping albedo of 0.91 at the entry to the pump duct are used. The neutral and ion fluxes at the core boundary are balanced and at the targets the Bohm-Chodura criterion is applied. It is important to note, that whilst the neutrals may interact with every surfaces, ions may only interact with surfaces where the grid intersects the vessel at the target plates. It is however, in principle, possible to apply chemical sputtering yields along the outer grid boundary. Physical

sputtering is implemented according to the Roth-Bohdansky formula and chemically sputtered carbon (where activated) is, in a simplistic assumption, released as atoms and not as hydrocarbons. Transport coefficients for $D_\perp$ and $\chi_\perp^{e,i}$ vary radially in the range of $0.2m^2/s$ to $1.0m^2/s$. It has been shown in [3], testing several volumetric and surface processes inside the computational domain of the grid, that the code package qualitatively simulates partially detached divertor conditions when matching experimental upstream profiles in the SOL reasonably well. Furthermore for the lowest density case with the drift terms activated it is possible to quantitatively achieve relatively well matched target profiles at the inner and outer targets simultaneously as compared to cases not including drift terms, Fig. 1, even though at the inner target the profile is slightly shifted. When increasing n_e^{sep} in the simulations code and experiment quickly diverge, especially at the inner target, where the trend of a decreasing Γ_{it}^{pk} cannot be reproduced even qualitatively. An experimentally not observed chemical sputtering yield, Y_{chem}, of 10% is required at the inner target to drop the particle flux considerably. However, even then does the code simulate a Γ_{it} that is too high compared to the experiment. Complete detachment at the inner target with rising $\bar{n}_e$ along with the strong asymmetry of Γ_t are not reproduced. It is concluded in [3] that in the modelling for $\bar{n}_e$ higher than the lowest density case, the radiative power and momentum exhaust are not sufficient.

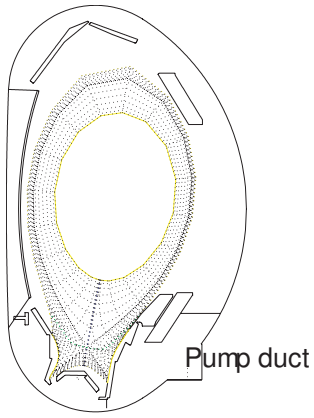

Figure 2: *Poloidal cross section of the magnetic configuration for* #21303@3.6*s represented by the corresponding grid that has been used for the simulations*

However, a possible candidate for exhausting sufficient power in the inner divertor to enhance momentum and charge removal may be in AUG the influx of intrinsic impurities from the heat shield at the high field side, HFS, [4, 5]. The radial ion out flux to the grid boundary and the impinging flux of neutrals onto the walls that produce intrinsic impurities could themselves depend on the divertor conditions due to neutrals escaping the divertor volume or neutrals plugged below the magnetic axis on the HFS because of the small gap. Therefore in an attempt to validate what the impact of the impurity influx from the HFS may be, instead of self-consistently calculating the carbon influx from the HFS PFCs on the basis of the modelled radial particle out flux, a carbon gas puff source is considered. The location of the puff is on the HFS above the inner divertor baffle outside of the computational grid and the injection is directed towards the grid with an opening angle of 45°. Carbon does not recycle on PFCs. The influx was varied from $5 \times 10^{18} s^{-1}$ to $1.3 \times 10^{21} s^{-1}$. In the modelling the background plasma directs the injected carbon towards the inner target. Only for carbon influxes larger than $1.6 \times 10^{20} s^{-1}$ a reduction of Γ_{it} of more than 20% is obtained at high densities. However, influxes larger than $6.5 \times 10^{20} s^{-1}$ increasingly affect the outer target unfavorably. According to Fig. 3 a radiative distribution that is closer to the experimentally observed can be obtained without invoking unrealistic Y_{chem} at the inner target plate when applying a carbon influx that is within the experimental margins, here $1.6 \times 10^{20} s^{-1}$. Moreover, as the simulated T_e profiles at the inner target are within the error

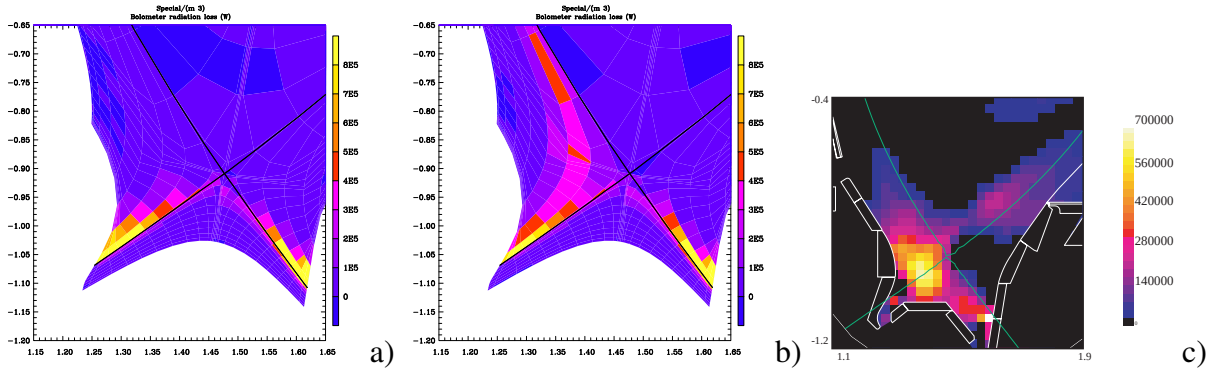

Figure 3: *Simulated radiation distribution without carbon (a) and with carbon influx* ($1.6 \times 10^{20} s^{-1}$) *(b) from the HFS together with experimental bolometric reconstruction (c)*

bars of Langmuir probe measurements the comparison of the simulated and experimental $2D$ radiative distribution for bolometry and for the D_α imaging diagnostic [6] allows to distinguish the simulation with drifts ($B25E$ drifts) from that with additional C influx from the HFS ($B25E$ C HFS) and drifts in Fig. 1. The HFS impurity influx reduces T_e not only close to the strike point, common to cases when assuming a high Y_{chem} at the target, but also radially into the far SOL and poloidally towards the X-point, thereby reducing the peak radiation value and increasing the radiative volume. Thus the case with impurity influx from the HFS is closer to overall experimental observations. However, only by introducing higher than experimentally observed impurity influxes can Γ_{it}^{pk} be dropped by a factor ~ 2 when n_e^{sep} is increased. Due to the colder divertor volume at the highest simulated impurity influxes, neutrals leaking across the separatrix on the HFS can increase n_e^{sep}.

Conclusions

Carbon sources and carbon transport play a key role for quantitatively understanding divertor detachment and the ion flux asymmetry observed between the inner and outer targets. Decisive new insight may be expected from the ongoing experimental campaign in a full tungsten machine. Detachment can be influenced by impurity sources that lie outside of the computational grid and self consistent modelling becomes challenging. The experimentally observed C influx from the HFS is a promising candidate at medium to high $\bar{n}_e$ for qualitatively and quantitatively explaining complete detachment along the inner target. However, only by applying carbon influxes that are larger than those experimentally observed can Γ_{it} be dropped by a factor ~ 2. The total carbon influx into the divertor needs to be determined and the role of supra-thermal electrons on the radiation efficiency of the impurity content remains unclear. Furthermore the perpendicular transport of impurities in the divertor is unknown and may depend on the charge state, Monte Carlo impurity transport codes such as DORIS or IMPMC may be required to determine the $2D$ distribution. The role of hydrocarbons larger than CD_4 needs to be investigated.

This work was supported by the U.S. Department of Energy under W-7405-ENG-48.

References

[**1**] R. Schneider et al., CPP **40**, 328 (2006). [**2**] M. Groth et al., these proceedings. [**3**] M. Wischmeier et al., Plasma Edge Theory 11, submitted to CPP. [**4**] R. Neu et al., JNM **363-365**,52 (2007).
[**5**] T. Pütterich et al., PPCF **45**, 1873 (2003). [**6**] J. Herhausen et al., these proceedings.